Inductance Calculation and Torque Separation of a Unique Multi-Layer Spoke-type Interior Permanent Magnet Motor using the Frozen Permeability Method

Inductance Calculation and Torque Separation of a Unique Multi-Layer Spoke-type Interior Permanent Magnet Motor using the Frozen Permeability Method

Hayder Abdulrahem
University of Thi-Qar
Nasiryah, Iraq
Email:
hayder.alrubyee@gmail.com

Patrick Chi-Kwong Luk
School of Water, Energy and Environment (SWEE)
Cranfield University
Bedfordshire, U. K
Email: p.c.k.luk@cranfield.ac.uk

Mohammed K. Al-Saadi
Electromechanical Engineering Dept
University of Technology
Baghdad, Iraq
Email:
mohammed16377@gmail.com

Abstract—Frozen permeability approach (FP) is employed to separate the average torque components (reluctance and permanent magnet torque) and for the inductance calculation for a Unique Ferrite Multi-Layer Spoke-type Interior Permanent Magnet Motor. Finite element analyses (FEA) models are built to provide many results help to offer more insight analysis. Three factors are taking in account to analyse their effects: permanent magnetism, armature currents of stator and angular rotor position. Also, different saturation levels are analysed, to reveal the influence of magnetic saturation and crosscoupling. These detailed analyses are providing valuable insights for permanent machine design and optimization.

Keywords— interior permanent magnet; Frozen permeability method; torque separation; nonlinear magnet, inductance calculations.

1. Introduction

The energy efficiency of a rotating electric machine and the torque/power density are an essential requirement. Recently, significant effort has been delivered to enhance the efficiency even with a small fraction without losing the torque density. Due to dramatically development in computational power the need for efficiency improvement, the Permanent magnet synchronous machines (PMSMs) are gaining the most increasingly attractive in various applications to be promising alternative due their high-power density, higher efficiency and exceptional control ability [1-3].

A comprehensive understanding and modelling of the torque component and flux distribution including saturation and crosscoupling effect production mechanism are required to accurately predict the performance of such an electric machine. In case of on-load PM or armature field, its essential to calculate the average torque separation, the flux density or flux linkage components. Existing research papers have been reported three methods have been reported in describing the average torque separation methods [*1-3*]: 1) the constant PM flux linkage model; 2) the partial-coupling model [*1*], in which the PM flux linkage restricted to axis current changing only; and 3) the frozen permeability (FP) FE method. Since the PM and armature fields influence each other and change with the magnetic saturation and crosscoupling, both the constant PM flux linkage model and the partial-coupling model may result in significant inaccuracy. Hence, the FP method is often employed [*4*] in order to accurately separate the PM and armature fields and hence the torque components accounting for the magnetic saturation and crosscoupling.

In this paper, inductance flux and the average torque components separated are calculated by the analytical model and compared and when the FP method is employed. Different values of average torque components have been calculated using these two methods. The average torque separation can be implemented properly with the FP method, while the analytical model cannot. The analysis has been done using inset of PM prototype machine, which is described in Section 2-1. The FP method is

illustrated, and the procedure of the on-load field components separation are introduced and analysed in Section 2-2. The field separation is examined and compared in normal FE in Section 3-1 Analyses for the total torque calculation and for the average torque separation in Section 4. Finally, the key point are highlighted in Section 6.

2. Background

2.1. Proposed Machine

PMSMs are one of must promising machine due to its high torque density and efficiency comparing to the IMs, However, As the future supply of rare-earth materials is likely to be limited because of the strategical nature, the prices of rare-earth materials and highly unstable in the global market. Ferrite magnets are representing the most alternative potential for non-rare-earth PMSMs to replace the IMs. For ferrite motor, since the eddy current loss in PM poles is eliminated and eddy loss of armature winding is negligible, overall eddy loss is extremely low. Moreover, the coreless in the rotor is reduced due to the non-conductive ferrite pole layers. In this work a 2kW two-layer spoke-type ferrite prototype machine is used to evaluate the impact of both crosscoupling and magnetic saturation, as well as the PM variation and reluctance torque components. A commercial version of induction machine with a power of 1.5kW and 36 slots with 4 poles is utilized in our work to provide housing and stator of our prototype machine. Starting from the analytical models with the help of optimization algorithm, results in a design of 6 poles rotor, while the stator windings are re-winded using single layer distributed windings based on short-pitch winding [6]. Fig. 1 (a)&(b) illustrates the cross-section of the machine model as well as the 3-D model of the prototype machine respectively. The specifications and dimensions are detailed in table I. Two magnets (PM2) are added to form a V-shape in between two first layer PMs to reduce the use of PM material and improve the reluctance torque. The current is three phases ideal sinusoidal and the current phase with a maximum amplitude=8.8A and the advance angle (phi) is varied from 0 to 90 The q axis current iq is positive and the d axis id current is negative.

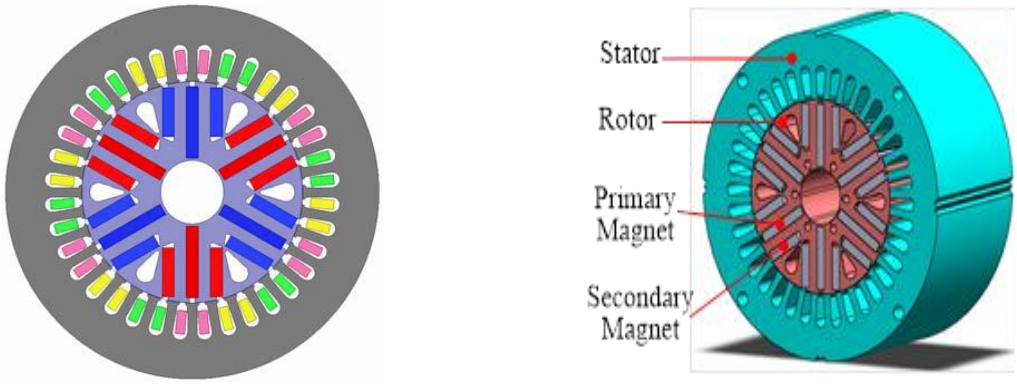

(a) FEA mode l(b) 3D model

Fig. 1. The proposed machine configuration

TABLE I GENERAL SIZING PARAMETERS

Parameters	***Value***	***Unit***
Stator Outer Diameter (Dso)	160	mm
Rotor Outer Diameter (Dro)	94.5	mm
Air gap Length (g)	0.25	mm
Stack Length (l)	90	mm
Base Rotating Speed	1500	rpm
Number of Poles (p)	6	

TABLE I GENERAL SIZING PARAMETERS

Parameters	***Value***	***Unit***
Number of Slots (q)	36	
Lamination Material	50CS470	
Torque	16	N.m
Rated speed	1500	rpm
PM Material	Y30	

2.2. Frozen Permeability Principle and Procedure

The principle of The FP method used to investigate the issues related with magnetic saturation and crosscoupling is illustrated in Fig 2 and will described in [1]

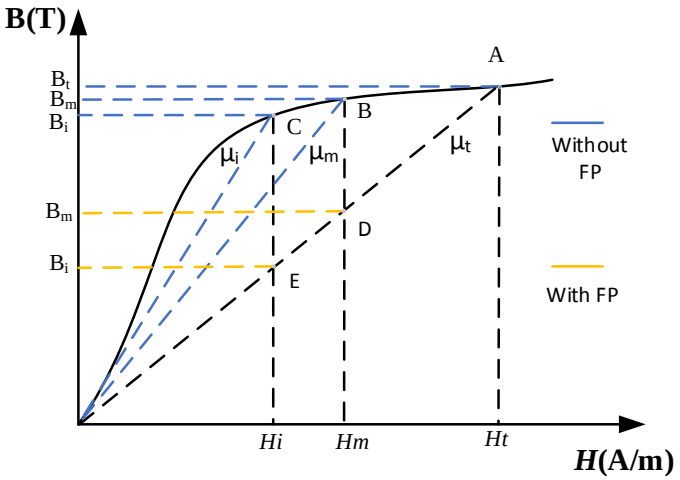

Fig. 2. Principle of frozen permeability method

Based on excluding FP method, and using only the PM excitation (H_{PM}), i.e., open circuit, this will make the resultant flux density is B_{PM} (point B). Also, the resultant flux density is Bi (point C) when the armature excitation (Hi) only. When the PM machine is working on load (point A), it is excited by both PM and current, i.e., $H_{all}=H_{PM}+H_i$. However, the resultant flux density Ball is lower than $B_{PM}+B_i$. It is not possible to decompose the on-load PM and armature field components. When using the FP method, firstly, μ_{all} and the on-load permeability is obtained and stored based on the on-load model (point A). Then, points D and E which are modeled by two linear analyses, can be solved. This solution is based on the frozen μ_{all} with one of two components, either the PM or armature excitation only to obtain B (FP, PM) or B (FP, i) respectively. The difficulty of nonlinear problem has been overcome by approximate it into linear one using freezing the permeability as µall, B_{all}=B (FP, PM) +B(FP,.i). This approximation helps to decompose the on-load PM and armature field components. Furthermore, we are including the influence of magnetic saturation and crosscoupling because μ_{all} varies according to the operation point. Fig. 3. Summarizes the procedure of the FEA computation which is based on the principle of the FP method.

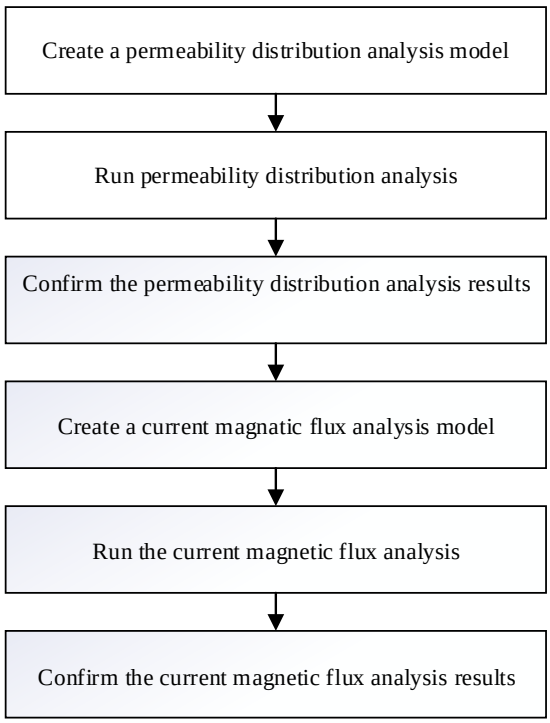

Fig.3. The procedure to obtaining the results

3. Analytical Calculations

3.1. Magnetizing inductances calculations

The saliency and reluctance torque are calculated after the d- and q-axis inductance have been calculated. In this work, starting with building analytical models. This model is used to evaluate the novel two-layer spoke-type ferrite IPM machines. The model has used to predict the armature reactions for prototype machine. The prediction is implemented based on the equivalent magnetic circuit theory in the d-q frame. the d-axis and q-axis magnetizing inductance can be obtained by:

$$\begin{cases} L_{md} = \frac{\Psi_{md}}{i_d} = \frac{4N_a R_{ro} l_{ef}}{p \cdot i_d} \sum_{v \neq m \cdot k} \frac{k_{wv}}{v} B_{gdv} = \sum_{v \neq m \cdot k} L_{mdv} \\ L_{mq} = \frac{\Psi_{mq}}{i_q} = \frac{4N_a R_{ro} l_{ef}}{p \cdot i_q} \sum_{v \neq m \cdot k} \frac{k_{wv}}{v} B_{gqv} = \sum_{v=6k\pm1} L_{mqv} \end{cases} \quad (1)$$

To reveal the influence of flux distribution with different harmonic orders, their contributions to the q-axis magnetizing inductance are listed in Table II.

Table II MAGNETIZING INDUCTANCE CALCULATIONS

Harmonic order	**magnetizing inductance calculations**		
	Analytical Lmd	***Analytical Lmq***	***Analytical Uf***
Total	0.01381484	0.090871165	0.277662023

The analytical inductance values are considering to be constant under different operating conditions. Much higher reluctance torque can be expected because of high Lq/Ld salient ratio, while the one-layer machine will be majorly of torque components dependent on PM torque

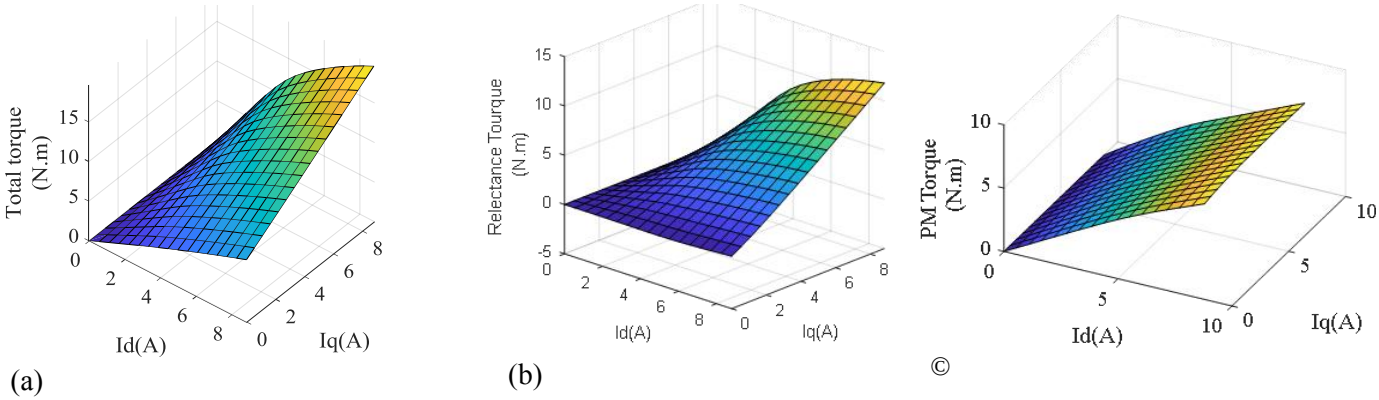

(a) (b) ©

Fig. 4. Torque profiles against id and iq by FEA (a) total torque (b)reluctance torque (c) PM torque.

3.2. Torque Production

The Permanent magnet motor has two components of electromagnetic torques: 1. The first torque component is PM. This component is resulting from the interactions between the field comes from armature windings and PM, 2. the second torque component is reluctance torque. This component is arising by the winding inductance changing with the rotor position due to the rotor saliency. The total torque production for a PMSM is calculated by [8]

$$\begin{cases} T_{pm} = \dfrac{mp}{4}\Psi_f i_q \\ T_r = \dfrac{mp}{4}(L_d - L_q) i_d i_q \end{cases} \qquad (2)$$

Ferrite PM machine cannot achieve high torque density because of its low magnetic strength as compared to PM torque density the rare-earth counterpart. To improve the torque density, a larger difference between the d- and q-axis inductances is needed as indicated in the second term inside the brackets of Equation (1). Fig. 4. illustrates the changes of average torque components with the current. At high currents values (high id and high iq), the overall electromagnetic torque performances of the Machin are expected to be different from real values due to heavily saturated working condition. The results reveal that the increase of armature current, the reluctance torque will grow more quickly than PM torque. Consequently, the contribution of the two torque components could be quite different under different loading conditions.

4. Simulation Results

4.1. Field Distributions

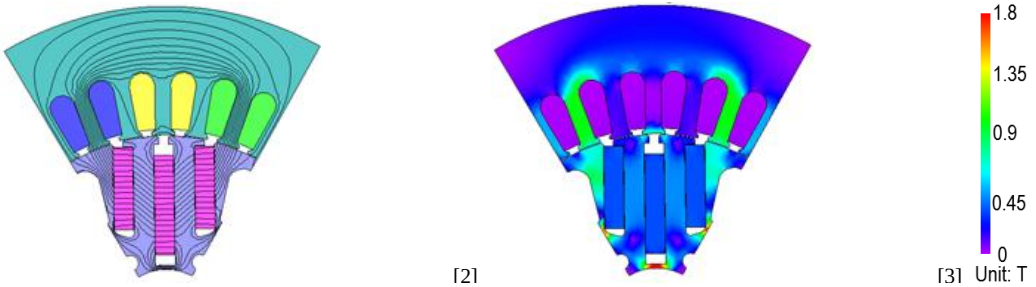

[1] [2] [3]

[4] (a) . [5] (b) [6]

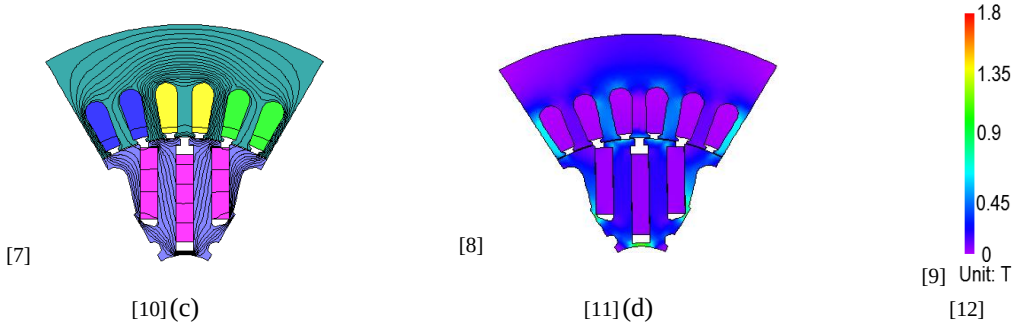

Fig. 5. field distributions when id=4.4A &iq=0A, 0. (a) and (b) whole field (current and PM) and (c) and (d) armature field current (FP)

Under on-load condition PM and armature field components can be calculated using the FP method. Fig 5 shows a contour plot of the magnetic flux density distribution and magnetic flux lines when the peak phase current is id=4.4 A, iq=0 A, and rotor position is 0 (electrical), results shows that the permeability distributions are not symmetrical in both d and q exes and the field distribution is asymmetrical accordingly. In Fig. 4(a) and (b) the influence of armature field can be seen. Therefore, the on-load PM field Fig. 4 (c) is asymmetric with the d-axis and has q-axis flux linkage, although the PM excitation

4.2. Magnetizing inductances calculations

Practically, the saturation and crosscoupling effects led to

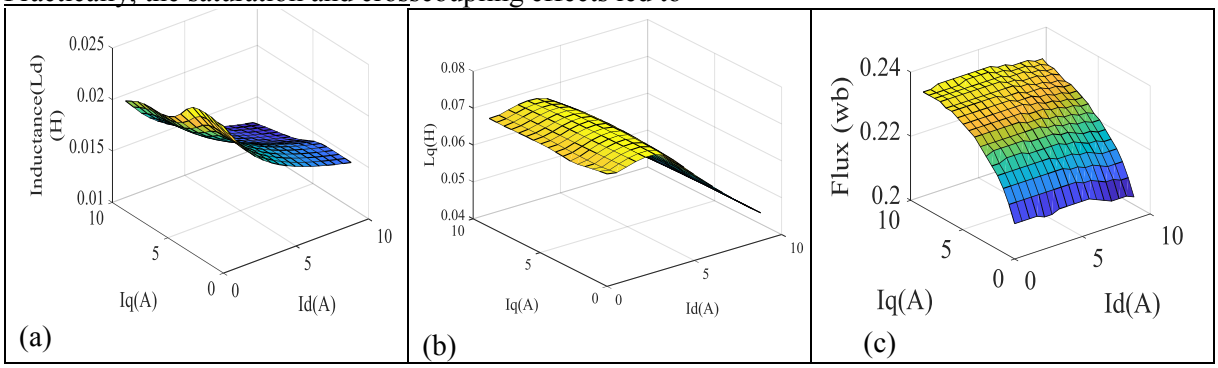

Fig. 6 Flux linkage and inductance of FEA (a)Lmd (b)Lmq (c)Uf

a change in these values. Fig6 demonstrates the variation of average flux linkages and inductances with the id and iq obtained by using FP method.

Fig 6-a shows that the Lmd affected more by id values than iq. For example, when iq was 1.65A, the Lmd has change from 0.023 to 0.018 when id varied from 0 to 8.8A.

5. Torqu Profile Predictions

5.1. Torque Production

The variation of average torque components with the

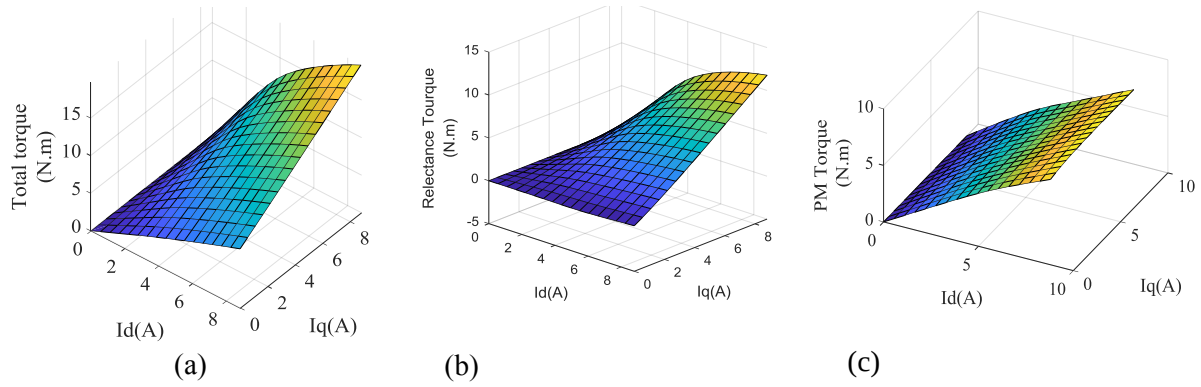

Fig. 7. Torque profiles against id and iq by FEA (a) total torque (b)reluctance torque (c) PM torque..

current resultant from FEA is shown in Fig. 7. T_{pm} and T_r are

influenced by the magnetic saturation. The (PM) torque component increase and become higher by increasing id. While it is less sensitive to the change in iq values. For example, when iq=1.1

Under zero id current, results show that The PM torque is almost identical for both models (analytical and FEA). This result can be representing the accuracy PM flux prediction. However, there is a slight difference between two model's reluctance torque because q-axis flux linkage and inductance are slightly lower than the FEA simulation. This difference will result in lower torque for the analytical method with the increase of id and machine loading. As a consequence, the error will increase because of saturation effect. The error will be n=more noticeable under heavy load conditions. The error may go up to 14% of the maximum torque output under severe saturation condition as depict in Fig. 5. However, with higher current angle, larger demagnetizing injected current the saturated is alleviated. Again, the predicted torque by analytical models coincides back with FEA. The trend of torque profile and the optimal current angle can be well predicted as compared with analytical, in spite of the error percentage increase with saturation. This good prediction can be very helpful for the preliminary design

6. Conclusion

In this paper, using the frozen permeability method, a model for the average torque separation and inductance calculating for novel two-layer spoke-type ferrite IPM machines are built. Firstly, FEA models are built and several simulations run under different load conditions to investigate the influences of the saturation and crosscoupling on the machine performances are deeply investigated. The developed procedure can offer overview design guidance for this developed type. Magnitude and phase of the current generate torque in an IPM motor. To enhance torque develop3ment large saliency ratio and flux focusing structure is designed which can provide similar portions of reluctance and PM torque Finally, various loading conditions is applied to the two-layer spoke-type ferrite IPM machine to validate the design by comparing test results with the derived analytical methods and torque performance.

References

[1] S. Javadi and M. Mirsalim, "Design and Analysis of 42-V Coreless Axial-Flux Permanent-Magnet Generators for Automotive Applications," IEEE Trans.Magn., vol. 46, no. 4, pp. 1015–1023, 2010.

[2] E. Sulaiman, T. Kosaka, and N. Matsui, "High Power Density Design of 6-Slot-8-Pole Hybrid Excitation Flux Switching Machine for Hybrid Electric Vehicles," IEEE Trans.Magn., vol. 47, no. 10. pp. 4453–4456, 2011.

[3] Z. Q. Zhu and D. Howe, "Electrical Machines and Drives for Electric, Hybrid, and Fuel Cell Vehicles," in Proc. the IEEE, vol. 95, no. 4. pp. 746–765, 2007.

[4] A. M. El-Refaie, "Fractional-slot concentrated-windings synchronous permanent magnet machines: Opportunities and challenges," IEEE Trans. Ind. Electron., vol. 57, no. 1, pp. 107–121, Jan. 2010.

[5] Z. Q. Zhu, “Fractional slot permanent magnet brushless machines and drives for electrical and hybrid propulsion systems,” Int. J. Comput.Math. Electr. Electron. Eng., vol. 30, no. 1, pp. 9–31, 2011.
[6] D. G. Dorrell, M. Hsieh, and A. M. Knight, “Alternative rotor designs for high performance brushless permanent magnet machines for hybrid electric vehicles,” IEEE Trans. Magn., vol. 48, no. 2, pp. 835–838, Feb. 2012.
[7] Bing Xia, Weizhong Fei and P. Luk, "Analysis and design of V-spoke ferrite interior permanent magnet machine for traction applications," 6th International Conference on Power Electronics Systems and Applications (PESA), Hong Kong, 2015, pp. 1-6
[8] Xia B., Luk PC. Analytical Model of Open-Circuit Characteristics of Two-Layer Spoke-Type Ferrite Interior Permanent Magnet Machines,IEEE International Electric Machines & Drives,Miami,USA,May 21-24,2017. IEEE International Electric Machines & Drives,Miami,USA,May 21-24,2017..
[9] Fei, W., D. Wu, B. Xia, and P.C.K. Luk. "Design of a multi-layer interior ferrite permanent magnet synchronous machine for traction applications", 7th IET International Conference on Power Electronics Machines and Drives (PEMD 2014), 2014.
[10] A.Wang, Y. Jia, and W. L. Soong, “Comparison of five topologies for an interior permanent-magnet machine for a hybrid electric vehicle,” IEEE Trans. Magn., vol. 47, no. 10, pp. 3606–3609, Oct. 2011.